Available online at www.sciencedirect.com
SCIENCE DIRECT®
Coordination Chemistry Reviews 249 (2005) 1468–1475
COORDINATION CHEMISTRY REVIEWS
www.elsevier.com/locate/ccr

Review

Combination of redox- and photochemistry of azo-conjugated metal complexes

H. Nishihara *

Department of Chemistry, School of Science, The University of Tokyo, 7-3-1 Hongo, Bunkyo-ku, Tokyo 113-0033, Japan

Received 20 July 2004; accepted 15 November 2004
Available online 5 March 2005

Contents

Abstract

Recent studies on azobenzene-combined photochromic metal complexes in which the redox chemistry of the metal complex moiety and photochemistry of the azobenzene moiety are coupled, are reviewed. Tris(azobenzene-bound bipyridine)cobalt compounds, $[Co(p\text{-abbpy})_3](BF_4)_n$ and $[Co(m\text{-abbpy})_3](BF_4)_n$ ($n = 2$, 3) (*p*-dbbpy and *m*-dbbpy are 4-(4-(4-tolylazo)phenyl-2,2′-bipyridine and 4-(3-(4-tolylazo)phenyl-2,2′-bipyridine, respectively), undergo reversible *trans–cis* isomerization using a combination of the Co^{III}/Co^{II} redox change and single UV light (366 nm) irradiation exciting the π–π^* transition. The *trans–cis* conversion yield is higher for the meta isomers, $[Co(m\text{-abbpy})_3](BF_4)_n$, than for the *para* isomers, $[Co(p\text{-abbpy})_3](BF_4)_n$. The *trans–cis* photoisomerization behavior of 4-[4-(tolylazo)phenyl]-6,6′-dimethyl-2,2′-bipyridine, dmabbpy, is synchronized with coordination of the bipyridine moiety to copper, and the *trans*/*cis* isomerization can be controlled reversibly through the Cu^{II}/Cu^{I} redox process and single UV light (365 nm) irradiation. 3-Ferrocenylazobenzene (3-FcAB), undergoes reversible *trans–cis* isomerization using a single green light (546 nm) source and the ferrocenium/ferrocene redox change. These results indicate that several kinds of photo–redox combined multi-functionalities can be realized for the azo-conjugated transition metal complexes by tuning the interaction between the azo moiety and the metal complex unit.

Keywords: d–π Interaction; Azobenzene; Photoisomerization; Redox; Bipyridine complex; Ferrocene

1. Introduction

Azobenzene is a popular photochromic molecule, the structure and color of which change reversibly by photo-irradiation. It has attracted much recent attention due to the possibilities of its application to molecular photo-memory

* Tel.: +81 3 5841 4346; fax: +81 3 5841 8063.
E-mail address: nisihara@chem.s.u-tokyo.ac.jp.

0010-8545/$ – see front matter © 2004 Elsevier B.V. All rights reserved.
doi:10.1016/j.ccr.2004.11.009

and photo-switches [1–3]. The *trans*-to-*cis* isomerization of azobenzene occurs by irradiation to the π–π* band with UV light and the reverse *cis*-to-*trans* isomerization takes place by irradiation of the n–π* band with blue light [4–7]. Thus, it needs two light sources for reversible isomerization.

We have been interested in the combination of this photo-functional molecule with transition metal complexes that also exhibit interesting magnetic, optical and electronic properties, because multi-functional molecules can be created by the fusion of the two functional molecular units. In the azo-conjugated metal complexes, there are two interesting issues to be clarified; first, what are the effects of metal complex units on the isomerization, and second, what are the changes in physical properties of metal complex units caused by isomerization. For several years we have been studying several kinds of complex units containing the azo group in order to obtain answers to these issues, and have found several interesting phenomena that have not been discovered in regular organic azobenzenes [8–16]. In this article, three different azo-conjugated metal complex systems showing novel functionalities through the combination of redox- and photochemistry are reviewed.

2. Reversible photoisomerization using a single UV irradiation frequency and the Co^{III}/Co^{II} redox process in azobenzene-attached tris(bipyridine)cobalt complexes

The characteristic features of tris(bipyridine)cobalt are the occurrence of a reversible redox reaction of the Co^{III}/Co^{II} couple and the high stability of both the Co^{II} and Co^{III} complexes in air, together with negligible absorption bands in the visible region in the both oxidation states. The photoisomerization behavior of both Co^{II} and Co^{III} complexes was investigated in order to identify the effects of the oxidation state on the photoisomerization behavior.

Two azobenzene-attached bipyridine ligands, *p*-abbpy and *m*-abbpy, and their Co^{II} and Co^{III} complexes, $[Co(p\text{-abbpy})_3](BF_4)_n$ and $[Co(m\text{-abbpy})_3](BF_4)_n$ ($n = 2$, 3) were synthesized and their electrochemical and photochemical properties were studied [17,18]. Reversible Co^{III}/Co^{II} redox reactions were observed in the cyclic voltammograms of the *p*-abbpy complex at −0.15 V versus Fc^+/Fc and of the *m*-abbpy complex at −0.11 V. The UV–vis absorption spectra of *p*-abbpy, $[Co(p\text{-abbpy})_3](BF_4)_2$ and $[Co(p\text{-abbpy})_3](BF_4)_3$, showed π–π* bands due to the azo group at $\lambda_{max} = 345$ nm ($\varepsilon = 3.5 \times 10^4\ mol^{-1}\ dm^3\ cm^{-1}$), 360 nm ($1.1 \times 10^5\ mol^{-1}\ dm^3\ cm^{-1}$), and 374 nm ($9.7 \times 10^4\ mol^{-1}\ dm^3\ cm^{-1}$), respectively [17]. Upon irradiation of the dichloromethane solution of *p*-abbpy with UV light at 366 nm, the π–π* band decreased in intensity and the n–π* band of the azo group at 445 nm increased in intensity, showing a typical *trans*-to-*cis* isomerization of the azobenzene moiety. The back *cis*-to-*trans* reaction proceeded by irradiation with 445 nm light. The molar ratio of the *cis* form estimated from ^1H NMR spectra reached 92% in the photostationary state (PSS) of the 366 nm irradiation. The spectroscopic changes of both $[Co^{II}(p\text{-abbpy})_3](BF_4)_2$ and $[Co^{III}(p\text{-abbpy})_3](BF_4)_3$, in dichloromethane were essentially identical to the change of *p*-abbpy upon irradiation with 366 nm light for the *trans*-to-*cis* isomerization followed by irradiation with 445 nm light for the *cis*-to-*trans* isomerization, but the *cis* molar ratio in the PSS with 366 nm irradiation is very dependent on the Co oxidation state. Values of 40% and 4% were determined for the Co^{II} and Co^{III} complexes, respectively.

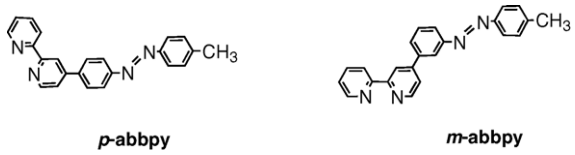

p-abbpy *m*-abbpy

The difference in the *cis* molar ratio in PSS between Co^{II} and Co^{III} indicates that *trans–cis* isomerization might be controlled, in either direction, with the same wavelength of light by changing the oxidation state between Co^{II} and Co^{III}. The following experimental results confirmed this idea. The dichloromethane solution of the trans form of $[Co^{II}(p\text{-abbpy})_3](BF_4)_2$ was irradiated with 366 nm light to reach PSS (Fig. 1a), and the resulting mixture of *trans* and *cis* forms was oxidized with a stoichiometric amount of 1,1′-dichloroferrocenium hexafluorophosphate, $[Fe(\eta^5\text{-}C_5H_4Cl)_2]PF_6$ ($E^{0\prime} = 0.19$ V versus Fc^+/Fc) in dark condition (Fig. 1b). The ratio of the *cis* form remained constant

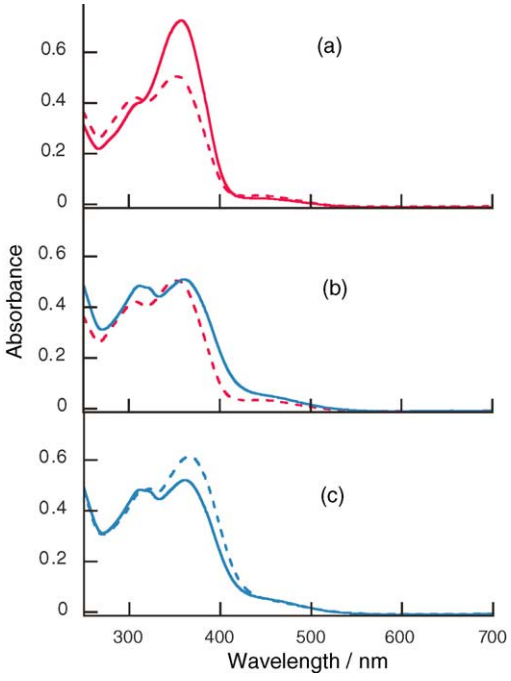

Fig. 1. Absorption spectroscopic changes of $[Co(p\text{-abbpy})_3](BF_4)_n$ in dichloromethane when the trans/Co(II) form was irradiated with 366 nm light (a), oxidized with $[Fe(\eta^5\text{-}C_5H_4Cl)_2]PF_6$ in the dark (b), and irradiated again with 366 nm light (c).

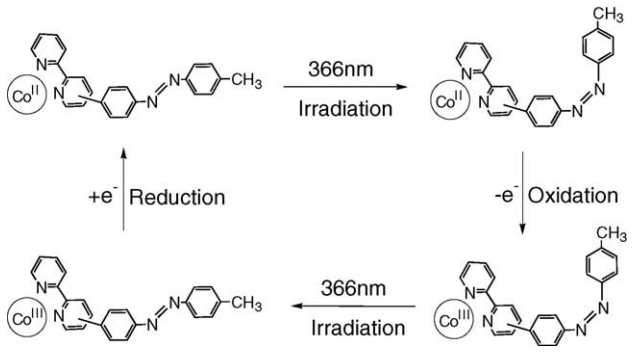

Scheme 1. Structures of *p*-abbpy, *m*-abbpy, $[Co(p\text{-abbpy})_3](BF_4)_n$, and $[Co(m\text{-abbpy})_3](BF_4)_n$.

after the oxidation, and the thermal isomerization to the trans form proceeded very slowly in the dark because the recovery of absorbance of the π–π^* band was not pronounced in intensity for more than 30 min. When the oxidized solution was exposed again to 366 nm light, the *cis*-to-*trans* photoisomerization promptly occurred to create the *trans*-rich PSS that was characteristic of the Co^{III} state, accompanied by a fast increase in the absorbance of the π–π^* band within a few minutes (Fig. 1c). The Co^{III} complex in PSS upon irradiation with 366 nm light was re-reduced with a stoichiometric amount of 1,1′-acetylcobaltocene, $[Co(\eta^5\text{-}C_5H_4COCH_3)_2]$ ($E^{0\prime} = -0.76$ V versus Fc^+/Fc), and exposure to the same 366 nm light resulted in a *trans*-to-*cis* isomerization to reach a different PSS that was characteristic of the Co^{II} state. These results suggest that a reversible *trans–cis* isomerization can be achieved in the *cis* molar ratio range of 4–40% by a combination of the reversible redox change between Co^{II} and Co^{III} and irradiation with a single UV light source; this is a novel route differing from the reversible isomerization of general organic azobenzenes with a combination of π–π^* and n–π^* excitation employing both UV light and visible light, respectively (Scheme 1) [17].

When we employed another series of compounds, *m*-abbpy, $[Co^{II}(m\text{-abbpy})_3](BF_4)_2$ and $[Co^{III}(m\text{-abbpy})_3](BF_4)_3$, an enhancement of the *cis* molar ratio range was accomplished [18]. Upon irradiation with 366 nm monochromatic light, the *cis* molar ratio reached 57% and 9% in PSS for $[Co^{II}(m\text{-abbpy})_3](BF_4)_2$ and $[Co^{III}(m\text{-abbpy})_3](BF_4)_3$, respectively. Thus, the difference between Co^{II} and Co^{III} is 48%, which is much improved from the 34% difference between the *p*-abbpy complexes. It is clear that this increase in the difference between Co^{II} and Co^{III} in *m*-abbpy complexes is based on the modulation of electronic interaction between the cobalt ion and the azo moiety. In both $[Co^{II}(m\text{-abbpy})_3](BF_4)_2$ and $[Co^{III}(m\text{-abbpy})_3](BF_4)_3$, the *cis* molar ratio generated by 366 nm light irradiation was doubled compared to that of the corresponding *p*-abbpy complexes, and the difference between Co^{II} and Co^{III} was increased. This is because both the Co^{II} and Co^{III} cations have an effect, through π-conjugation, of suppressing the *cis* formation of the azo moiety, and this effect can be weakened by *meta* substitution compared with *para* substitution. The *trans*-to-*cis* photoisomerization quantum yield, $\Phi_{t\rightarrow c}$ of $[Co^{II}(m\text{-abbpy})_3](BF_4)_2$ was 0.11, which is almost the same as that of azobenzene ($\Phi_{t\rightarrow c} = 0.10$), but lower than the value ($\Phi_{t\rightarrow c} = 0.07$) obtained for $[Co^{II}(p\text{-abbpy})_3](BF_4)_2$. This result has proven that coordination to a cobalt ion affects the azo π–π^* excitation state through an electronic interaction, suppressing the *trans*-to-*cis* isomerization efficiency. The effect seems to be more significant in the Co^{III} complexes than in the Co^{II} complexes. Preliminary transient absorption spectroscopy measurements with $[Co^{II}(m\text{-abbpy})_3](BF_4)_2$ and $[Co^{III}(m\text{-abbpy})_3](BF_4)_3$ following photoirradiation with 360 nm light has shown that the latter yields a spectrum with a 580 nm peak, which was not observed in the spectrum of the former which are similar to those of free *m*-abbpy [19]. This indicates the existence of an electron or energy transfer pathway from the photoexcited state of the azobenzene moiety to the Co^{III} center. The electron transfer pathway to form an azobenzene cation radical and a Co^{II} center is more likely because it is energetically possible; it has been reported that the azobenzene cation radical formed by flash radiolysis has a similar peak around 580 nm [20].

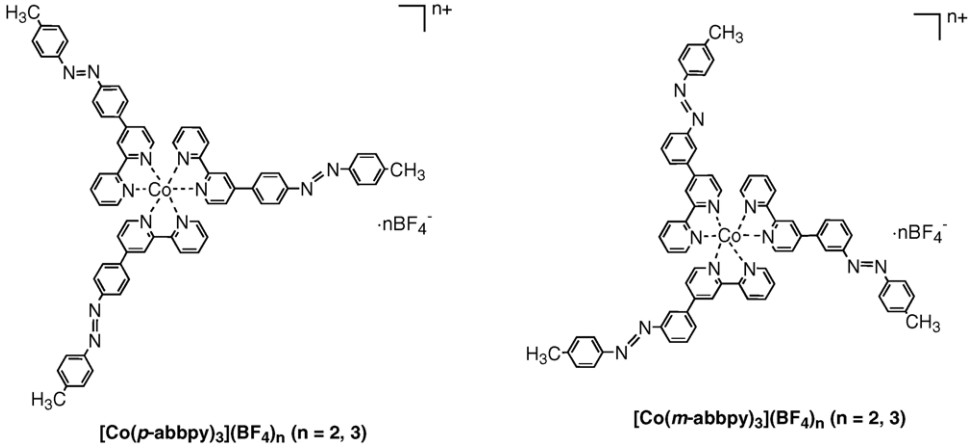

$[Co(p\text{-abbpy})_3](BF_4)_n$ (n = 2, 3) **$[Co(m\text{-abbpy})_3](BF_4)_n$ (n = 2, 3)**

In conclusion, reversible *trans–cis* isomerization has been achieved by a combination of the reversible redox reaction between Co^{II} and Co^{III} and a single UV irradiation frequency for azobenzene-bound tris(bipyridine)cobalt complexes. This

method should provide a new design for photochemical and electrochemical hybrid molecular systems.

3. Reversible photoisomerization of bipyridylazobenzene using a single UV irradiation frequency and driven by the Cu^{II}/Cu^{I} redox process and a ligand-exchange reaction

In contrast to cobalt, which favors hexa-coordinate tris(bipyridine) complexes as noted above, copper usually gives tetra-coordinate bis(bipyridine) complexes, whose geometry is interchanged between square planar Cu^{II} and tetrahedral Cu^{I} by the reversible redox reaction [21–23]. Recently, several molecular systems that incorporate a copper complex unit have been developed to induce molecular motions by electrochemical signals [24–26]. If the structural conversion causes a ligand exchange reaction, the condition of the ligand changes between coordinated and free forms, and thus the physical property of the ligand can be significantly altered. We applied this concept to the construction of a molecularly synchronized system in which the *trans–cis* isomerization of azobenzene attached to a bipyridine ligand was controlled by its binding to, or release from copper driven by a Cu^{II}/Cu^{I} redox change [27].

A 6,6′-dimethyl-substituted, azobenzene-substituted bipyridine ligand, dmabbpy, was designed as a new photoactive and ligand-exchangeable molecule, and its Cu^{I} and Cu^{II} complexes $[Cu(dmabbpy)_2]BF_4$ and $[Cu(dmabbpy)_2](BF_4)_2$, respectively, were synthesized. Photoirradiation of the ligand dmabbpy at 365 nm causes effective *trans*-to-*cis* isomerization of the azobenzene moiety, yielding a 94% molar fraction of the *cis* isomer in PSS. On the other hand, the *cis* molar fractions at 365 nm in the PSS for the Cu^{I} and Cu^{II} complexes were 18% and 14%, respectively. It is speculated that retardation of *cis* formation would be caused by the effective energy or electron transfer from the excited azo π–π^* state to another state in both oxidized states. The *cis* yields imply that the change in the *cis* ratio in PSS by the redox change is less significant than that for the cobalt complexes $[Co(p\text{-abbpy})_3](BF_4)_n$ ($n = 2, 3$).

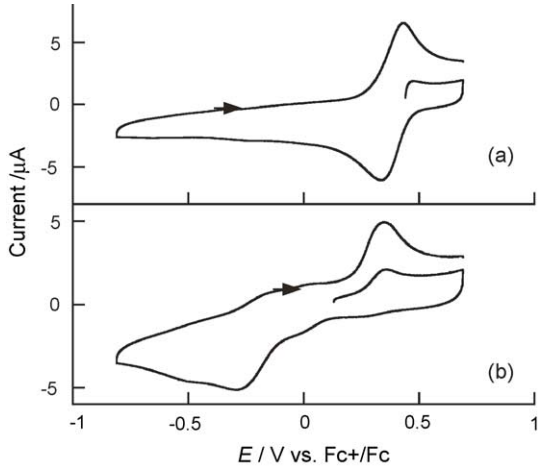

Fig. 2. Cyclic voltammograms of $[Cu(dmabbpy)_2](BF_4)_2$ in 0.1 mol dm^{-3} Bu_4NBF_4–CH_2Cl_2: in pure form (a), and mixed with two equivalents of bpy (b).

Fc^+/Fc in the cyclic voltammogram. The positive shift can be attributed to the effect of steric hindrance by the methyl groups in dmabbpy preventing the formation of a favorable square-planar structure in the Cu^{II} state [28].

Upon addition of two equivalents of bpy to the solution of $[Cu(dmabbpy)_2](BF_4)_2$, the oxidation wave to Cu^{II} in the cyclic voltammogram, appeared at 0.32 V, similar to that without bpy, whereas the reduction wave to Cu^{I} at ca. 0.3 V disappeared and a new wave was observed at −0.30 V (Fig. 2). Judging from these potentials, the major complex ion species existing in solution is $[Cu^{I}(dmabbpy)_2]^+$ in the Cu^{I} state and $[Cu^{II}(bpy)_2]^{2+}$ in the Cu^{II} state. Thus, a facile ligand exchange reaction has occurred on the time scale of cyclic voltammetry because both $[Cu^{II}(dmabbpy)_2]^{2+}/[Cu^{I}(dmabbpy)_2]^+$ and $[Cu^{II}(bpy)_2]^{2+}/[Cu^{I}(bpy)_2]^+$ couples undergo reversible redox reactions and appear independently in the electrolyte solution. The following UV–vis data support this consideration. When bpy was added to a solution of $[Cu(dmabbpy)_2](BF_4)_2$, the azo π–π^* band underwent a blue shift (352 nm). When five equivalents of bpy were added, the shift was saturated and the peak appeared at 345 nm, identical to the π–π^* band location of the free ligand, dmabbpy. In contrast, almost no shift in the azo π–π^* band occurred with the addition of bpy to a solution of $[Cu(dmabbpy)_2]BF_4$. The driving force of this reversible ligand exchange reaction can be attributed to the difference in coordination geometry between Cu^{I} and Cu^{II}.

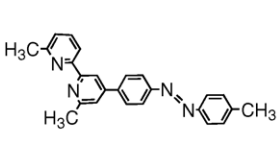

dmabbpy

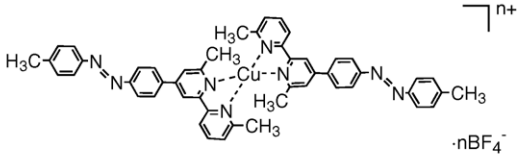

$[Cu(dmabbpy)_2](BF_4)_n$

In a cyclic voltammogram of $[Cu(dmabbpy)_2](BF_4)_2$ in Bu_4NBF_4-dichloromethane, a reversible Cu^{II}/Cu^{I} redox wave appeared at 0.37 V versus Fc^+/Fc. This value is considerably more positive than the redox potential of the non-substituted 2,2′-bipyridine (bpy) complex, $[Cu(bpy)_2]BF_4$ exhibiting a reversible redox wave at $E^{0\prime} = -0.12$ V versus

On the one hand, the Cu^{I} cation prefers the tetrahedral geometry, which is stabilized by the interlocking effect of the methyl groups in dmabbpy. On the other hand, when Cu^{I} is oxidized to Cu^{II}, the copper center prefers bpy, because the methyl groups in dmabbpy cause significant steric hindrance of the coordination of the Cu^{II} cation in the favored square-planar geometry.

The ligand exchange reaction caused by the Cu^{II}/Cu^{I} redox reaction noted above provides a mechanism to modify the photochemical properties of dmabbpy. Coordinated dmabbpy does not isomerize effectively but free dmabbpy undergoes efficient isomerization as mentioned above. Thus, we investigated the photoisomerization behavior of copper complexes in the presence of bpy. The absorption changes of a $[Cu^{I}(dmabbpy)_2]^{+}$ solution added with two equivalents of bpy upon UV irradiation exhibited significant differences compared with those of the $[Cu^{II}(dmabbpy)_2]^{2+}$ solution with two equivalents of bpy. These spectra suggest that the Cu^{I} solution gives a *trans*-rich composition in the PSS, while the Cu^{II} solution has a *cis*-rich composition using the same UV light irradiation (Fig. 3).

The *cis* molar ratio in the PSS (365 nm) was examined as a function of the amount of bpy added to the solution. In $[Cu^{II}(dmabbpy)_2](BF_4)_2$ solution, the *cis* molar ratio increased with addition of bpy, and the ratio saturated when two equivalents of bpy were added, whereas $[Cu^{I}(dmabbpy)_2]BF_4$ showed little increase of the *cis* form with the addition of bpy. Thus, when two equivalents of bpy were added, the cis molar ratios in the PSS for $[Cu^{I}(dmabbpy)_2]BF_4$ and $[Cu^{II}(dmabbpy)_2](BF_4)_2$ converted to 25% and 72%, respectively, from 18% and 14% in the absence of bpy.

Reversible photoisomerization with a single UV frequency with change in Cu^{II}/Cu^{I} was examined as follows. A mixture of $[Cu^{I}(dmabbpy)_2]BF_4$ and two equivalents of bpy in dichloromethane was irradiated with 365 nm light, forming 32% of the *cis* isomer. Then the same sample was oxidized to the Cu^{II} state with one equivalent of $[Fe(\eta^5\text{-}C_5H_4Cl)_2]PF_6$ and re-irradiated with the same 365 nm light; this resulted in

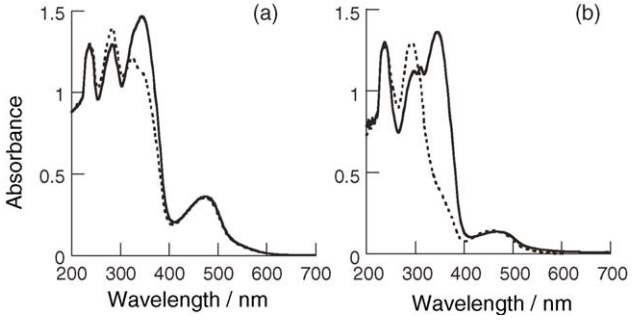

Fig. 3. UV–vis absorption spectroscopic changes of $[Cu(dmabbpy)_2]BF_4$ (2.0×10^{-5} mol dm^{-3}) plus bpy (4.0×10^{-5} mol dm^{-3}) (a), and $[Cu(dmabbpy)_2](BF_4)_2$ (2.0×10^{-5} mol dm^{-3}) plus bpy (4.0×10^{-5} mol dm^{-3}) (b) on photoirradiation in CH_2Cl_2. Solid and dotted lines refer to the all-*trans* form and the *trans*/*cis* mixture in the PSS at 365 nm, respectively.

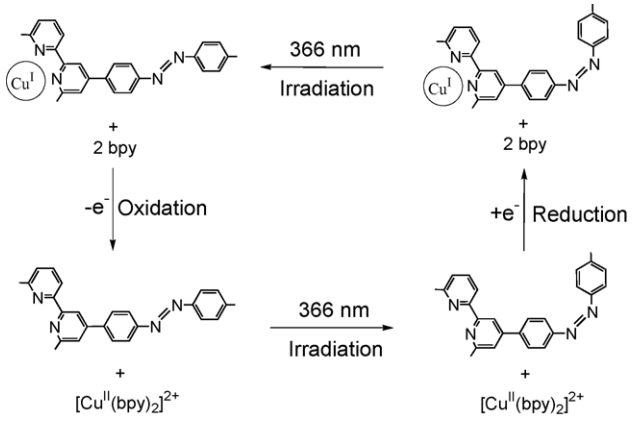

Scheme 2. Structures of dmabbpy and $[Cu(dmabbpy)_2](BF_4)_n$.

further *trans–cis* isomerization and an increase of the *cis* ratio to 70%. Then the copper was reduced to the Cu^{I} state with one equivalent of $[Co(\eta^5\text{-}C_5H_4COCH_3)_2]$ and re-irradiated with 365 nm light.

In conclusion, the *trans–cis* photoisomerization behavior of the azobenzene moiety was synchronized with ligand coordination of the conjugated bpy moiety to copper (Scheme 2). The coordination reaction can be reversibly controlled by changing the oxidation state of copper, leading to reversible *trans–cis* isomerization using a combination of UV light and redox reaction with a good *cis* isomer molar ratio [27]. The higher *cis* ratio with the reduced state of the metal center is opposite to the result described above for the cobalt complexes.

4. Reversible photoisomerization in 3-ferrocenylazobenzene using a single green light frequency and the ferrocenium/ferrocene redox process

Photoreaction by green light (546 nm) irradiation exciting a low-lying MLCT (metal-to-ligand charge transfer) band was discovered for azoferrocene [29,30], but the photoproduct is chemically reactive [31,32]. This prompted us to seek a more stable photoisomerization molecular system. We employed ferrocenylazobenzenes, one of which, 3-ferrocenylazobenzene, 3FcAB, exhibited reversible isomerization using only 546 nm irradiation in combination with the reversible redox reaction between ferrocene and ferrocenium (Scheme 3) [33].

Trans-3FcAB showed an azo π–π^* band at $\lambda_{max} = 318$ nm and a weak visible band at 444 nm. The azo π–π^* band decreased in intensity through green (546 nm) and UV light (320 nm) irradiation. These wavelengths correspond to the edge of the visible MLCT band and the maximum in the azo π–π^* band, respectively. The *cis* molar ratio estimated from ^{1}H NMR spectra reached 35% in the PSS upon 546 nm irradiation; the PSS was shown to be more *cis*-rich state (61%

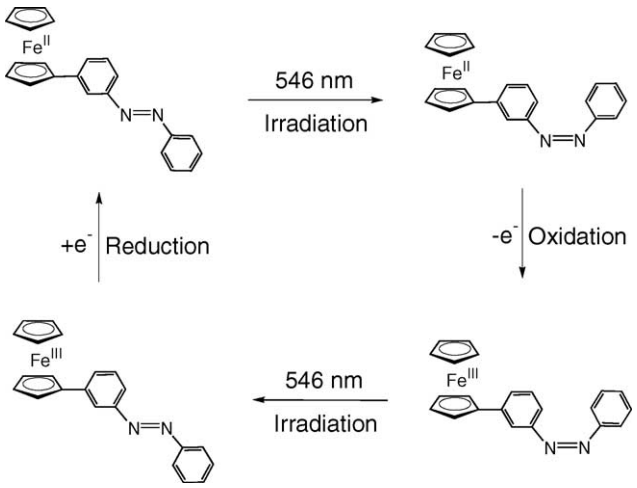

Scheme 3. Structures of 3FcAB and 4FcAB

Table 1
Cis molar ratios in the PSS of ferrocenylazobenzenes

	Excitation wavelength (nm)					
	320	350	436	500	546	600
3FcAB	61%		17%	36%	35%	
4FcAB		41%	6%	7%	6%	0%

cis molar ratio) upon the UV irradiation (see Table 1). The quantum yield for the *trans*-to-*cis* isomerization, $\Phi_{t\rightarrow c}$, of 3FcAB was estimated to be 0.51 for green light (546 nm), which is much higher than that (0.021) for UV light (320 nm) and exceeds that of azobenzene ($\Phi_{t\rightarrow c} = 0.12$ (313 nm excitation) [34]). The rate of decrease in the intensity of the π–π* band is similar for both 546 and 320 nm irradiation in Fig. 4, because the absorption of *trans*-3FcAB at 546 nm is much weaker than that at 320 nm while the quantum yield at 546 nm irradiation is much higher than that at 320 nm irradiation. The thermal *cis*-to-*trans* isomerization

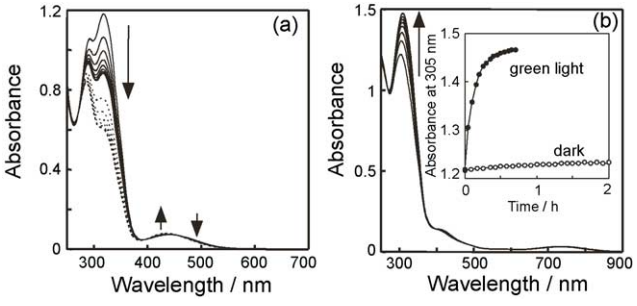

Fig. 4. (a) UV–vis absorption spectroscopic change of *trans*-3FcAB (5.52×10^{-5} mol dm^{-3}) in MeCN upon irradiation with 546 nm light for 21 min (solid lines) and subsequent irradiation at 320 nm for 4 min (dotted lines); (b) UV–vis absorption spectroscopic change of the following sample solution upon irradiation with 546 nm light, inset: time course change in absorbance at 305 nm of the sample solution upon irradiation with 546 nm light (solid circles) or in the dark (open circles). The sample solution was prepared by irradiation with a 546 nm light to *trans*-3FcAB in MeCN (5.62×10^{-5} mol dm^{-3}) to reach PSS and then oxidation with one equivalent of $[Fe(\eta^5\text{-}C_5H_4Cl)_2]PF_6$.

of 3FcAB, the rate constant of which $k = 1.3 \times 10^{-4}$ s^{-1} at 70 °C, was as slow as that of azobenzene ($k = 1.3 \times 10^{-4}$ s^{-1} at 70 °C).

Both the electrochemical oxidation and the chemical oxidation of *trans*-3FcAB with $[Fe(\eta^5\text{-}C_5H_4Cl)_2]PF_6$ from ferrocene to ferrocenium caused a shift of the π–π* band to higher energy from λ_{max} = 318 to 312 nm, then a weak LMCT band appeared at 730 nm. The completely reversible spectroscopic change indicated the high reversibility of the electrochemical ferrocenium/ferrocene redox reaction. Photoisomerization of the *trans*-ferrocenium state of 3FcAB was highly dependent on the irradiation wavelength. The decrease in absorbance of the π–π* band in the ferrocenium state observed under UV irradiation was almost entirely absent under 546 nm irradiation.

The possibility that single 546 nm irradiation might induce reversible *trans–cis* conversion by changing the oxidation state of the iron center was examined by the following experiments. An acetonitrile solution of *trans*-ferrocene form of 3FcAB was irradiated with 546 nm light to reach PSS (35% *cis* molar ratio), and the resulting *trans–cis* mixture was oxidized by addition of a stoichiometric amount of $[Fe(\eta^5\text{-}C_5H_4Cl)_2]PF_6$. After oxidation, recovery of the absorbance of the π–π* band was not pronounced in intensity over several hours in the dark at room temperature, and thermal isomerization to the trans form proceeded only very slowly in the ferrocenium state ($k = 8.7 \times 10^{-4}$ s^{-1} at 70 °C). Further 546 nm irradiation promoted an increase in the absorbance to reach the *trans*-rich PSS characteristic of the ferrocenium state, suggesting that almost all of the trans form was photo-recovered. These results indicate that the reversible *trans–cis* isomerization can be achieved by a combination of "on–off switching" of the MLCT character due to the redox change between ferrocene and ferrocenium and single green light irradiation. The LMCT band that appeared in the ferrocenium state is not associated with the isomerization.

The photoisomerization and thermal isomerization behavior of ferrocenylazobenzenes were strongly influenced by the substitution position of the ferrocenyl moiety on the benzene ring. *Trans*-4-ferrocenylazobenzene (*trans*-4FcAB) exhibited an intense visible MLCT band (494 nm) and an azo π–π* band (λ_{max} = 352 nm), which is largely red-shifted, compared to azobenzene (317 nm) or *trans*-3FcAB (318 nm). The *trans*-to-*cis* isomerization proceeded with $\Phi_{t\rightarrow c} = 0.0033$ by irradiation with UV light (350 nm) to reach a 41% *cis* molar ratio in the PSS. However, the MLCT in 4FcAB was not effective for the *trans*-to-*cis* conversion, whereas the *cis*-to-*trans* back reaction could be promoted even by orange light at 600 nm, which corresponds to the edge of the MLCT band, instead of blue light (~450 nm) (see Table 1). Fast recovery of the intensity of the π–π* band due to the transformation of the *cis* form into the trans form was observed immediately after the oxidation of the photo-generated *trans–cis* mixture at room temperature, indicating that the thermodynamic stability of the *cis* form was remarkably reduced by the oxidation

(the *cis*-to-*trans* thermal isomerization rate is $3.8 \times 10^3\ s^{-1}$ at 5 °C).

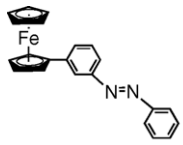

3fcab

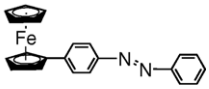

4fcab

It is of great interest that the 546 nm light caused a much higher *cis* molar ratio in 3FcAB than in 4FcAB and azobenzene. This problem was investigated by time-dependent density functional theory (TD-DFT) calculations for 3FcAB and 4FcAB in the trans form, in order to determine the singlet excited state in which the isomerization occurs. The calculated excitation energies in the *trans* forms were in reasonable agreement with the experimental values, and the observed trends in the experimental absorption spectra were reasonably reproduced (see Table 2). Noticeable features in the nature of the excited states of the *trans*-3FcAB are that the azo n–π^* strongly mixes with the MLCT state, and that the initial orbital for the 3.02 eV MLCT state is delocalized over Fe and the Cp ring rather than localized on the iron. The presence of MLCT character is the reason that the molar extinction coefficient of the visible band ($\lambda_{max} = 444$ nm, $\varepsilon = 1.86 \times 10^3\ mol^{-1}\ dm^3\ cm^{-1}$) is much larger than that of the n–π^* band of *trans*-azobenzene ($\lambda_{max} = 444$ nm, $\varepsilon = 5.15 \times 10^2\ mol^{-1}\ dm^3\ cm^{-1}$). The origin of the visible band in 3FcAB is different from that of 4FcAB, because the initial orbital for the 2.51 eV MLCT state of the latter is localized on the iron. The 546 nm light-induced *trans*-to-*cis* isomerization of 3FcAB may occur on the potential energy surface for the MLCT excited state. In fact, the almost complete absence of a response to the 546 nm light for the *cis* formation in the ferrocenium state is caused by the disappearance of the MLCT character in the ferrocene state by oxidation to ferrocenium (Fig. 5).

Table 2
Experimental and theoretical[a] excitation energies to the lowest excited state among those of similar character

Excitation energy (eV)		Oscillator strength (theoretical)	Assignment (CI coefficient)[b]
Experimental	Theoretical		
trans-3FcAB			
–	2.43	0.001	Azo n–π^* (0.55) + ML (azo π^*)CT (−0.33)
2.79	3.02	0.060	ML (azo π^*) CT (0.65)
3.90	3.49	0.693	Azo π–π^* (0.59)
cis-3FcAB			
–	2.45	0.047	Azo n–π^* (0.56) + ML (azo π^*) CT (−0.21)
–	3.16	0.001	ML (azo π^*) CT (0.35) + Cp-azo π^* (0.31)
–	3.96	0.103	Azo π–π^* (0.58)
trans-4FcAB			
–	2.42	<0.001	Azo n–π^* (0.66)
2.51	2.63	0.113	ML (azo π^*) CT (0.57)
3.52	3.03	0.752	Azo π–π^* (0.55)

[a] TD-DFT calculations with three-parameterized Becke–Lee–Yang–Parr (B3LYP) hybrid exchange-correlation functional.
[b] The expansion coefficient for the excited-state wave function.

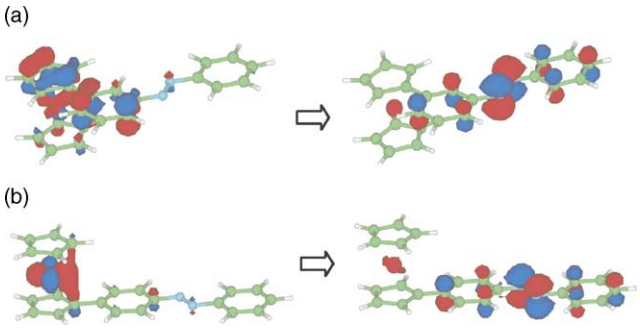

Fig. 5. The molecular orbitals contributing to the MLCT of *trans*-3FcAB (a) and *trans*-4FcAB (b).

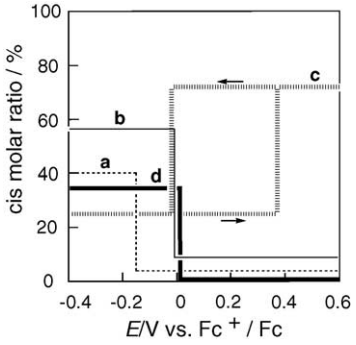

Fig. 6. Electrochemical potential dependence of the cis molar ratio in the PSS of $[Co(p\text{-abbpy})_3]^{3+/2+}$ upon 366 nm irradiation (a), $[Co(m\text{-abbpy})_3]^{3+/2+}$ upon 366 nm irradiation (b), $[Cu(dmabbpy)_2]^{2+/+}$ plus bpy upon 365 nm irradiation (c), and 3FcAB upon 546 nm irradiation (d).

5. Conclusion

Three different systems comprising azo and transition metal complex moieties that can undergo redox-conjugated photoisomerization were summarized in Fig. 6. They show unique behavior that has not been seen in common organic azo compounds. To observe such behavior, appropriate electronic and/or steric interactions between the azo and complex moieties them are important. No multi-functionality appears when the interaction is too weak, and their original functions are perturbed too much when the interaction is too strong. The approach used here to create new types of photochromic materials with multi-mode functions via properly designed azo-conjugated metal complexes might be applicable to the combination of other metal complexes and other photochromic molecules.

Acknowledgements

The author thanks the following people who worked on the present study: co-workers at the University of Tokyo are Dr. Masato Kurihara, Dr. Shoko Kume, Akira Hirooka, Kyoko Yamaguchi, and Dr. Masaki Murata; collaborators are Prof. Manabu Sugimoto at Kumamoto University and Prof. Naoto Tamai at Kwansei University. This work was supported partly by Grants-in-Aid from the Ministry of Education, Culture, Sports and Science of Japan, and The 21st Century COE Program for Frontiers in Fundamental Chemistry.

References

[1] M. Irie, Chem. Rev. 100 (2000) 1683.
[2] T. Ikeda, O. Tsutsumi, Science 268 (1995) 1873.
[3] S. Kawata, Y. Kawata, Chem. Rev. 100 (2000) 1777.
[4] H. Rau, in: H. Dürr, H.B. Laurent (Eds.), Photochromism: Molecules and Systems, Elsevier, Amsterdam, 1990, p. 165 (Chapter 4).
[5] H. Rau, Angew. Chem. Int. Ed. Engl. 12 (1973) 224.
[6] N. Tamai, H. Miyasaka, Chem. Rev. 100 (2000) 1875.
[7] M. Kojima, T. Takagi, T. Karatsu, Chem. Lett. (2000) 686.
[8] T. Yutaka, M. Kurihara, H. Nishihara, Mol. Cryst. Liq. Cryst. 343 (2000) 193.
[9] T. Yutaka, I. Mori, M. Kurihara, J. Mizutani, K. Kubo, S. Furusho, K. Matsumura, N. Tamai, H. Nishihara, Inorg. Chem. 40 (2001) 4986.
[10] T. Yutaka, I. Mori, M. Kurihara, N. Tamai, H. Nishihara, Inorg. Chem. 42 (2003) 6306.
[11] T. Yutaka, M. Kurihara, K. Kubo, H. Nishihara, Inorg. Chem. 39 (2000) 3438.
[12] T. Yutaka, I. Mori, M. Kurihara, J. Mizutani, N. Tamai, T. Kawai, M. Irie, H. Nishihara, Inorg. Chem. 41 (2002) 7143.
[13] M. Nihei, M. Kurihara, J. Mizutani, H. Nishihara, Chem. Lett. (2001) 852.
[14] M. Nihei, M. Kurihara, J. Mizutani, H. Nishihara, J. Am. Chem. Soc. 125 (2003) 2964.
[15] M. Kurihara, H. Nishihara, Coord. Chem. Rev. 226 (2002) 125.
[16] H. Nishihara, Bull. Chem. Soc. Jpn. 77 (2004) 407.
[17] S. Kume, M. Kurihara, H. Nishihara, Chem. Commun. (2001) 1656.
[18] S. Kume, M. Kurihara, H. Nishihara, J. Korean Electrochem. Soc. 5 (2002) 189.
[19] S. Kume, K. Yamaguchi, N. Tamai, H. Nishihara, unpublished results.
[20] K. Daasbjerg, K. Sehested, J. Phys. Chem. A 106 (2002) 11098.
[21] G.C. Percy, D.A. Thornton, J. Mol. Struct. 14 (1972) 313.
[22] J. Foley, S. Tyagi, B.J. Hathaway, J. Chem. Soc., Dalton. Trans. (1984) 1.
[23] M. Munakata, S. Kitagawa, A. Asahara, H. Masuda, Bull. Chem. Soc. Jpn. 60 (1987) 1927.
[24] M.H. Al-Sayah, N.R. Branda, Chem. Commun. (2002) 178.
[25] N. Armaroli, V. Balzani, J.-P. Collin, P. Gaviña, J.-P. Sauvage, B. Ventura, J. Am. Chem. Soc. 121 (1999) 4397.
[26] G. De Santis, L. Fabbrizzi, D. Iacopino, P. Pallavicini, A. Perotti, A. Poggi, Inorg. Chem. 36 (1997) 827.
[27] S. Kume, M. Kurihara, H. Nishihara, Inorg. Chem. 42 (2003) 2194.
[28] P. Federlin, J.-M. Kern, A. Rastegar, New J. Chem. 14 (1990) 9.
[29] M. Kurosawa, T. Nankawa, T. Matsuda, K. Kubo, M. Kurihara, H. Nishihara, Inorg. Chem. 38 (1999) 5113.
[30] M. Kurihara, T. Matsuda, A. Hirooka, T. Yutaka, H. Nishihara, J. Am. Chem. Soc. 122 (2000) 12373.
[31] M. Kurihara, T. Matsuda, A. Hirooka, T. Yutaka, H. Nishihara, J. Am. Chem. Soc. 126 (2004) 4740 (Erratum for Ref. [28]).
[32] Y. Men, Ph.D. thesis, The University of Tokyo, 2002.
[33] M. Kurihara, A. Hirooka, S. Kume, M. Sugimoto, H. Nishihara, J. Am. Chem. Soc. 124 (2002) 8800.
[34] H. Rau, J. Photochem. 26 (1984) 221.